C. R. Physique 11 (2010) 405–410

Contents lists available at ScienceDirect

Comptes Rendus Physique

www.sciencedirect.com

Optical properties of nanotubes / Propriétés optiques des nanotubes

# Opto-electrical characterization of infrared sensors based on carbon nanotube films

## *Caractérisation électro-optique de détecteurs infrarouge à base de films de nanotubes de carbone*

Charlie Koechlin [a,b,*], Sylvain Maine [b], Stéphanie Rennesson [a,b], Riad Haidar [a], Brigitte Trétout [a], Annick Loiseau [c], Jean-Luc Pelouard [b]

[a] *Onera, chemin de la Hunière, 91761 Palaiseau, France*
[b] *Laboratoire de photoniques et nanostructures (LPN-CNRS), route de Nozay, 91461 Marcoussis, France*
[c] *Laboratoire d'étude des microstructures, UMR 104 ONERA-CNRS, ONERA BP72, 92322 Châtillon cedex, France*

ARTICLE INFO

*Article history:*
Available online 9 September 2010

*Keywords:*
Carbon nanotubes
Infrared sensor
Resistance dispersion

*Mots-clés :*
Nanotubes de carbone
Détecteur infrarouge
Dispersion des caractéristiques

ABSTRACT

A large array of devices based on a carbon nanotubes film was realized. Electrical characterization by the transfer length method enables the determination of the sheet resistance, and contact resistance, which is extremely low. The resistance dispersion is shown to be due to the film non-uniformity, and is low enough to enable the realization of bolometer focal plane arrays. A decrease of the resistance with the temperature is observed and leads to a *TCR* of $-0.2\%K^{-1}$. The strong absorption of carbon nanotubes films in the mid infrared transmission band (3–5 μm and of 8–14 μm) enables us to demonstrate the first carbon nanotubes photo response for these wavelengths.


RÉSUMÉ

Nous présentons ici la caractérisation électrique d'une matrice de dispositifs à base de film de nanotubes de carbone par la méthode TLM. Elle nous a permis de montrer que les résistances de contact obtenues étaient quatre ordres de grandeur en dessous de l'état de l'art. La dispersion des caractéristiques au sein de la matrice s'avère suffisamment faible pour être compatible avec la réalisation d'un imageur. Une décroissance de la résistance avec la température a été mesurée, et donne une *TCR* de $-0{,}2\%K^{-1}$. La forte absorption des films de nanotubes de carbone dans les bandes infrarouges de transmission atmosphérique (3–5 μm et 8–14 μm), nous a permis d'observer les premières photo-réponses à ces longueurs d'onde.


## 1. Introduction

Single-wall carbon nanotubes (SWCNTs) are attractive materials from both fundamental and technological points of view. Since their discovery, they have been mainly studied as individual objects especially in the nano-electronics domain [1,2].

* Corresponding author at: Onera, chemin de la Hunière, 91761 Palaiseau, France.
*E-mail address:* charlie.koechlin@onera.fr (C. Koechlin).

1631-0705/$ – see front matter 
doi:10.1016/j.crhy.2010.06.005

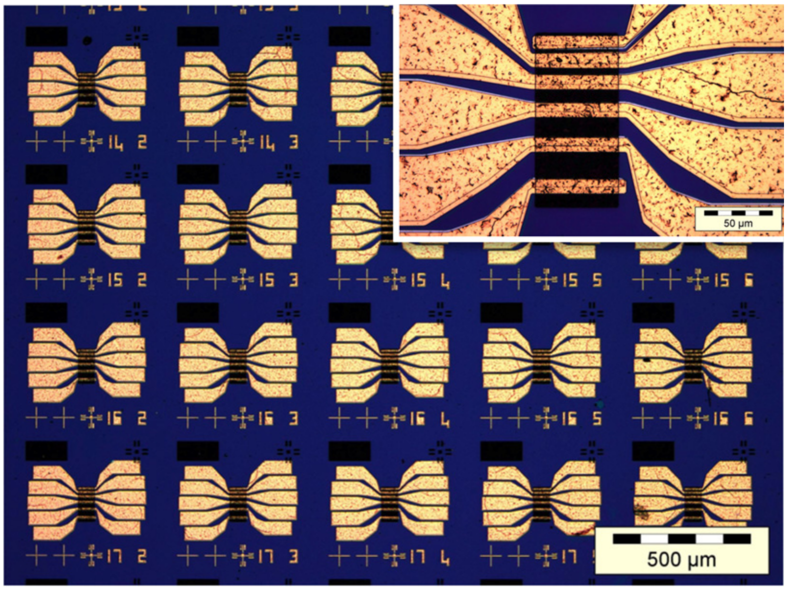


**Fig. 1.** Matrix of identical devices. Insert: Device with the 5 inter-electrodes spacing $d_i$ for TLM.

SWCNT field effect transistors already outperform the state-of-the-art silicon technologies in various figures of merit [3]. However, devices based on individual SWCNT have very poor reproducibility, and their fabrication techniques are not yet scalable for mass production. Moreover, it is currently impossible to obtain SWCNTs with a controlled chirality, and the connection of these nano structures to metal electrodes remains a challenge [4–6]. As a consequence the behavior of devices based on individual SWCNTs is unpredictable.

However, nanotube films make these difficulties disappear thanks to two characteristics: the ensemble averaging over a large number of tubes, and the large film area (typically at the semiconductor wafer scale). Thus SWCNT-films appear as a new material with unique electro-optical properties. They seem to be an appropriate candidate for flexible electronics [7], gas sensors [8], actuators [9], and transparent conductive electrodes [10]. Moreover, the much larger active areas of SWCNT-films compared to those of individual SWCNTs leads to a higher sensitivity for opto-electronic devices. Itkis et al. [11] demonstrated the first near infrared (IR) bolometer made of a suspended millimeter-size ribbon of a 100 nm-thick SWCNT-film. In this configuration when the absorbed IR radiation heats the film, a bolometric photo-signal is obtained, because its resistance highly depends on temperature.

Here we present the opto-electrical characterization of an array of SWCNT-film based devices. The opto-electrical response of such devices is based on the variation of the film conductivity. Thus the contact resistance must not hinder the film resistance. As a consequence we used the transfer length method (TLM) to extract both the average specific contact resistance, and the sheet resistance of the film. The I–V characteristics are investigated over the array as a spatial uniformity criterion. We have also studied their temperature dependence, which is essential for a bolometric sensor, and sheds light on the conduction mechanisms in the SWCNT-films. FTIR measurement of the transmission and reflection of carbon nanotube films shows an important absorbance of the SWCNT-films. A photo-response was also observed [12] in the mid-infrared atmospheric transmission bands (3–5 µm and 8–12 µm).

## 2. Device fabrication

Our SWCNT-films are fabricated as follows: SWCNTs are obtained from commercial sources (HiPCO) and their powders are dispersed in deionized water containing sodium cholate (used as surfactant). The solution is sonicated and centrifuged in order to separate the impurities from the SWCNTs. The solution is filtrated through a porous filtration membrane forming a homogeneous SWCNT-film [13], then the surfactant is washed away with deionized water, and finally the SWCNT-film is reported on the host wafer by dissolving the membrane (made of cellulose esters) with acetone.

Our samples are fabricated in four main steps [12]. First UV-patterned platinum electrodes are deposited by lift-off on a silica on silicon wafer using an e-beam evaporator. Then, as previously described a 200-nm-thick film of SWCNTs is deposited over the metallic electrodes. Next, the film is structured by $O_2$ plasma in an inductively coupled plasma (ICP) system in order to define the active regions. Finally a second set of electrodes is deposited on top of the CNT mesa, and is aligned with the first one. An array of 360 identical devices (Fig. 1) is fabricated on each sample. A single device, consisting of a ribbon of SWCNTs mesa (width $W = 60$ µm) contacted with six double electrodes (width $L = 5$ µm) defining five various spacing of length $d_i$ for TLM, is shown on the inset of Fig. 1.

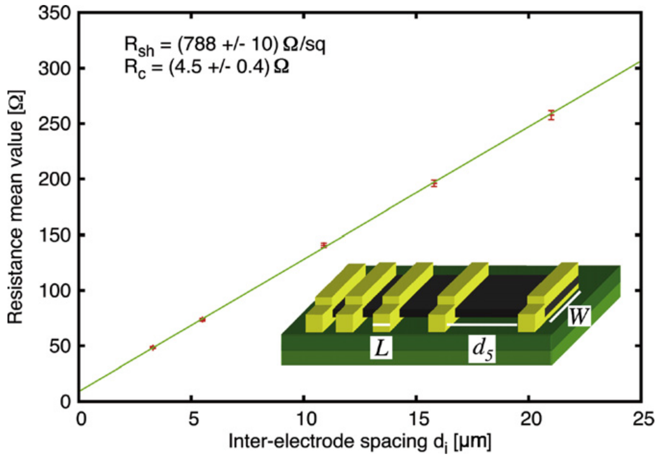


**Fig. 2.** Average resistance $\langle R_i \rangle$ of each spacing versus their length $d_i$ with error bars. The curve is the fit obtained with Eq. (1). Insert: Structure of a single device.

**Table 1**
Measured ohmic contact parameters and comparison with Ref. [10].

| | Metal | $R_{sh}$ (Ω/sq) | $R_c$ (Ω) | $L_T$ (µm) | $\rho_c$ (Ω cm$^2$) |
|---|---|---|---|---|---|
| Present work | Pt | $788 \pm 10$ | $4.5 \pm 0.4$ | $0.38 \pm 0.04$ | $(1.1 \pm 0.1) \times 10^{-6}$ |
| Ref. [10] | Ag | 350 | 2.8 | 80 | $2 \times 10^{-2}$ |

## 3. Electrical characterization

The total resistance $R_i$ for a given spacing ($d_i$) is:

$$R_i = 2R_c + R_{sh} \cdot \frac{d_i}{W} \tag{1}$$

where $R_c$ is the contact resistance between the film and the metal electrodes, and $R_{sh}$ the sheet resistance. The current flowing through the SWCNT-film is transferred to the metallic contacts over the characteristic length $L_T$. Thus the contact resistance reads:

$$R_c = \frac{R_{sh} L_T}{W} \coth(L/L_T) \tag{2}$$

One can also determine the specific contact resistance, $\rho_c = R_{sh} L_T^2$ which is the common geometry-independent figure of merit.

Four-probe measurements of the five spacings $d_i$ were carried out over the 360 devices of the sample. The average resistance $\langle R_i \rangle$ for each spacing $d_i$ is shown on Fig. 2. A linear fit with Eq. (1) enables to extract $R_{sh}$ and $R_c$, from which $L_T$ and $\rho_c$ are deduced (see Table 1). Our technological process improves the specific contact resistance of about four orders of magnitude compared to previous work [10]. The likely explanation is the better ability of platinum to provide efficient electrical contacts as well as the quality of the interface between the SWCNT-film and the contact electrodes. A small specific contact resistance appears as a significant improvement for bolometric applications. Indeed the contact length ($W$) could be reduced in order to increase the thermal isolation of the film and the contact width ($L$) could be submicronic (i.e. a few $L_T$ from Eq. (2)) in order to increase the device density, especially for focal plane array applications.

Since our process provides a large number of devices, we can measure the dispersion of their characteristics. Fig. 3 represents, for each inter-electrode spacing $d_i$, the distribution of the total resistance measured through the array. The relative dispersion is small (about 15%) but the absolute value grows with $d$. A further data processing ($R_{sh}$ and $R_c$ distributions) indicates that $R_{sh}$ is the main cause for dispersion. That is the reason why the dispersion is larger for longer spacings. In a focal plane array, there is a need for uniformity between the pixels; our measurements confirm that our devices dispersion is sufficiently low to be compatible.

In order to investigate the temperature dependence of electrical characteristics, we performed TLM measurements on a single device for various temperatures. The contact resistance $R_c$ appears to be temperature-independent (in the uncertainties range), while $R_{sh}$ strongly decreases with temperature (Fig. 4). This decrease was already observed by other authors [11,14–17]. Nevertheless, they did not extract the sheet resistance of their films, so the role of contacts was still a matter of debate.

Bolometric responsivity is defined by the resistance variation due to a heating. The corresponding figure of merit is the temperature coefficient of resistance ($TCR$), which is defined by:

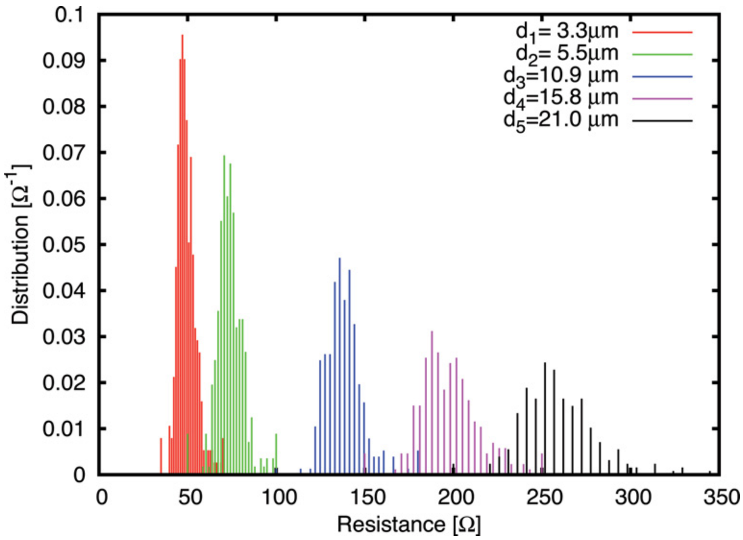


**Fig. 3.** Distribution of the resistances measured among the 360 devices for each electrodes spacing $d_i$.

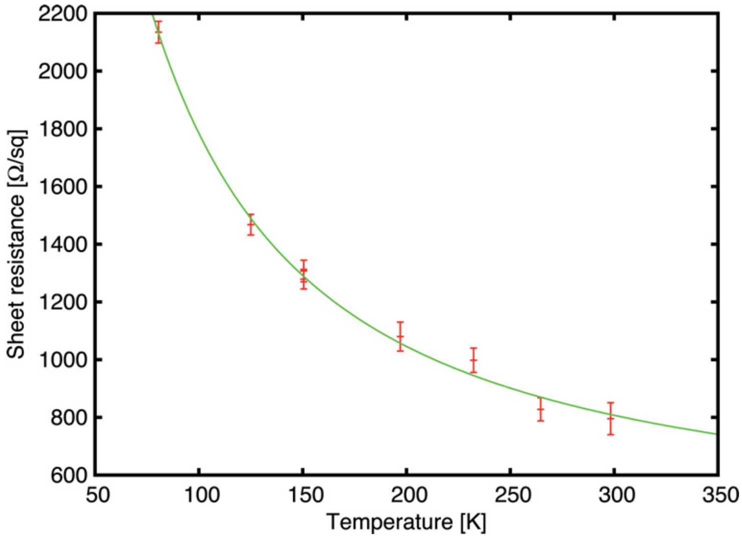


**Fig. 4.** Sheet resistance with error bars versus temperature.

$$TCR = \frac{1}{R}\frac{\mathrm{d}R}{\mathrm{d}T} \tag{3}$$

For our SWCNT-film, *TCR* is found to be equal to $-0.2\%\mathrm{K}^{-1}$ at room temperature, which is close to data previously published for purified SWCNTs (without any special treatments to enhance the *TCR*) by Itkis et al. [11]: $\approx 0.1\%\mathrm{K}^{-1}$ (for a 1-µm-thick film) or by Lu et al. [18]: $-0.07\%\mathrm{K}^{-1}$ (for a 90-nm-thick film). These values are lower than those of conventional IR bolometers [19] based on amorphous silicon or vanadium oxides (*TCR* around $-2.5\%\mathrm{K}^{-1}$). However Lu et al. [18] demonstrated its improvement by thermal annealing and chemical functionalization.

Nevertheless the TCR, is not the only relevant parameter involved in the responsivity which is defined for a constant bias as:

$$\Re(A/W) = \frac{\eta.TCR\,V_{bias}}{G_{th}.R} \tag{4}$$

where $\eta$ is the absorption coefficient, $V_{bias}$ is the applied voltage, and $G_{th}$ is the thermal conductance describing the coupling of the membranes with its environment. It appears that an important criterion is $TCR/R$. In the case of amorphous silicon the $TCR/\rho$ (with $\rho$ the resistivity) value is $-0.033\%/\mathrm{K}\,\Omega\,\mathrm{cm}$ [20] because of its high resistivity. For our SWCNT-films this parameter is found to be equal to $-12\%/\mathrm{K}\,\Omega\,\mathrm{cm}$. So even if they have a lower *TCR*, they present a promising $TCR/\rho$ ratio. It means that we can expect, if all other parameters are equal, a great enhancement of the responsivity.

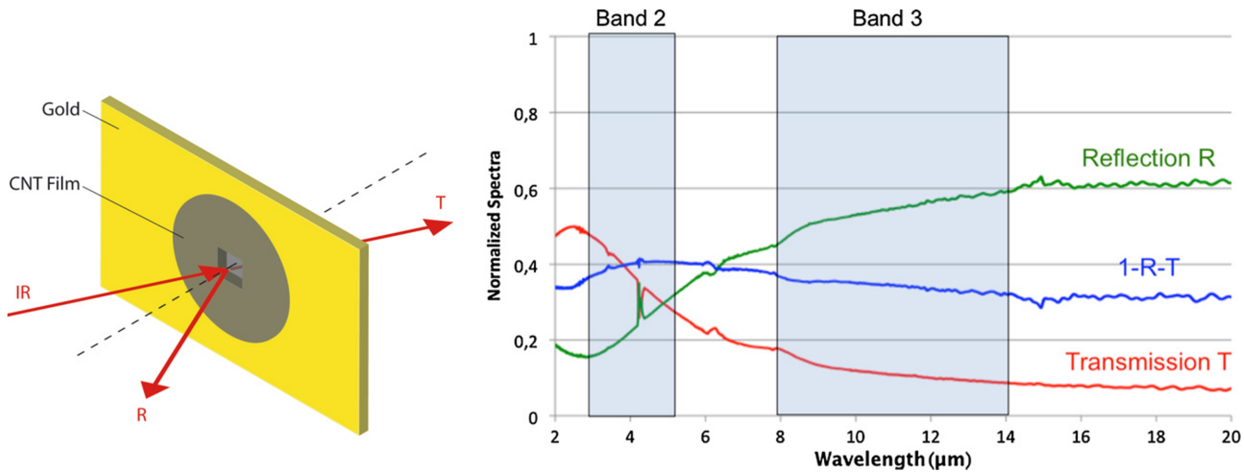


**Fig. 5.** Reflection ($R$) and transmission ($T$) IR spectra of a suspended SWCNT-film (thickness 350 nm) for an incidence of 13°.

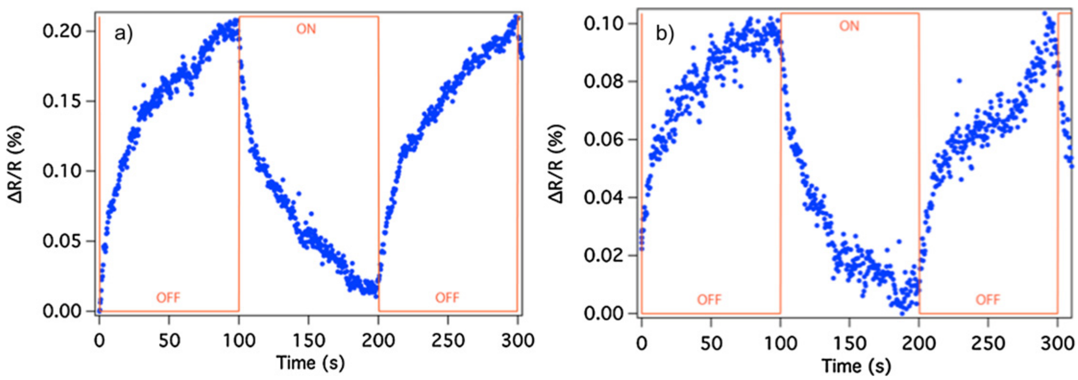


**Fig. 6.** a) Variation of the resistance as a function of time in the range 3–5 µm with an irradiance of 100 mW/cm$^2$ and b) variation of the resistance as a function of time in the range 9–18 µm with an irradiance of 10 mW/cm$^2$.

## 4. FTIR measurements

The near infrared spectra of SWCNT-films have been intensively studied over the last decade due to the presence of the Van Hoove singularities. Itkis [11] demonstrated the first IR bolometer based on SWCNTs in these wavelengths. However, poor attention has been paid to the mid infrared properties, even if there is a huge potential in these range especially in thermal imaging applications. We performed FTIR measurements on a SWCNT film suspended over a hole. The obtained transmission ($T$) and reflection ($R$) spectra are presented on Fig. 5 for an incidence of 13°. SWCNT-films appear to have a flat absorbance (defined as $A = 1 - R - T$) of 30% between 3 and 20 microns. This is very relatively high for materials, which are only few hundreds of nanometers thick, and could be enhanced using a quarter wavelength resonator.

The origin of this absorbance of SWCNT-film was addressed by Itkis et al. [21] and attributed to an intra-band transition due to hole doping for the semi-conducting tubes and to the presence of a mini gap for the metallic ones which is an effect of the curvature. These results pave the way to a mid infrared sensor based on SWCNT-films because of the absorption in the atmosphere transmission windows (band 2 and 3).

## 5. Photo-response

In our devices the SWCNT-film is lying on the substrate. As a consequence, it is not an appropriate configuration to observe a bolometric effect. Indeed, even if the SWCNT-film absorbs the incoming infrared radiation, it heating will remain low due to the thermal coupling with the substrate, and the responsivity will be also low. In the same way, because the film transfers its thermal energy to the substrate, the response time will be high because of its thermal inertia. Nevertheless we performed photo-response measurements on such structures. A black body at 1100 °C is used to enlight our sample on which a constant bias is applied (100 mV) at room temperature. Optical pass band filters in the 3–5 µm and of 9–18 µm tanges are successively intercalated between the sample and the black body leading to an irradiance of respectively 100 mW/cm$^2$ and 10 mW/cm$^2$.

Fig. 6 shows a relative resistance modulation ($\Delta R/R$) of 0.2% and 0.1% with a response time of several minutes. Even if the responsivity is quite low, and the response time too long, these results are the first demonstration, of a photo-response in the infrared atmospheric transmission windows for SWCNT-materials. In order to enhance the performance the SWCNT-film must be suspended.

## 6. Conclusion

As a conclusion, a large array of devices based on a SWCNT-film was realized. Platinum contacts on this film provide specific contact resistance as low as $1.1 \times 10^{-6}$ ohm cm$^2$, i.e. an improvement of four orders of magnitude as compared to previous works [10]. The resistance dispersion is shown to be due to the film non-uniformity, and is low enough to enable the realization of bolometer focal plane arrays. A decrease of the resistance with the temperatures is observed and leads to a *TCR* of $-0.2\%\text{K}^{-1}$. The strong absorption of SWCNT-films in the mid infrared transmission band (3–5 μm and of 8–14 μm) enables us to demonstrate the first SWCNTs photo response for these wavelengths. Efforts are currently made in order to be able to suspend our micro bolometers and therefore enhance their performances. These systems appear as promising candidates for low cost uncooled focal plane array for IR or even THz detection [21].

## Acknowledgements

The authors would like to acknowledge support by the Délégation Générale pour l'Armement.

## References

[1] S.J. Tans, A.R.M. Verschueren, C. Dekker, Nature 393 (1998) 49–52.
[2] R. Martel, T. Schmidt, H.R. Shea, T. Hertel, Ph. Avouris, Appl. Phys. Lett. 73 (1998) 2447–2449.
[3] P. Avouris, Z. Chen, V. Perebeinos, Nat. Nanotech. 2 (2007) 605.
[4] Y. Nosho, Y. Ohno, S. Kishimoto, T. Mizutani, Nanotech. 17 (2006) 3412–3415.
[5] T. Kanbara, T. Takenobu, T. Takahashi, Y. Iwasa, K. Tsukagoshi, Y. Aoyagi, H. Kataura, Appl. Phys. Lett. 88 (2006) 053118.
[6] D. Mann, A. Javey, J. Kong, Q. Wang, H. Dai, Nano Lett. 3 (2003) 1541.
[7] D. Zhang, K. Tyu, X. Liu, E. Polikarpov, J. Ly, M.E. Tompson, C. Zhou, Nano Lett. 6 (2006) 1880.
[8] P. Bondavalli, P. Legagneux, D. Pribat, Sensors and Actuators B: Chemical 140 (2009) 304–318.
[9] S. Lu, B. Panchapakesan, Appl. Phys. Lett. 88 (2006) 253107.
[10] R. Jackson, S. Graham, Appl. Phys. Lett. 94 (2009) 012109.
[11] M.E. Itkis, F. Borondics, A. Yu, R.C. Haddon, Science 312 (2006) 413.
[12] S. Maine, C. Koechlin, R. Fleurier, R. Haidar, N. Bardou, C. Dupuis, B. Attal-Trétout, P. Mérel, J. Deschamps, A. Loiseau, J.-L. Pelouard, PSSC, in press.
[13] Z. Wu, Z. Chen, X. Du, J.M. Logan, J. Sippel, M. Nikolou, K. Kamaras, J.R. Reynolds, D.B. Tanner, A.F. Hebard, A.G. Rinzler, Science 305 (2004) 1273.
[14] A.B. Kaiser, G. Düsberg, S. Roth, Phys. Rev. B 57 (1998) 1418.
[15] V. Skákalová, A.B. Kaiser, U. Dettlaff-Weglikowska, K. Hrnčariková, S. Roth, J. Phys. Chem. B 109 (2005) 7174–7181.
[16] E. Bekyarova, M.E. Itkis, N. Cabrera, B. Zhao, A. Yu, J. Gao, R. Haddon, J. Am. Chem. Soc. 127 (2005) 5990.
[17] V. Skákalová, A.B. Kaiser, Y.-S. Woo, S. Roth, Phys. Rev. B 74 (2006) 085403.
[18] R. Lu, G. Xu, J.Z. Wu, Appl. Phys. Lett. 93 (2008) 213101.
[19] A. Rogalski, Prog. Quan. Elec. 27 (2003) 59–210.
[20] J.J. Yon, in: Proceeding of International Symposium OPTRO 2010, Paris, France.
[21] M.E. Itkis, S. Niyogi, M.E. Meng, M.A. Hamon, H. Hu, R.C. Haddon, Nano Lett. 2 (2002) 155.